42nd AIAA Thermophysics Conference
27 - 30 June 2011, Honolulu, Hawaii

AIAA 2011-4027

An Inverse Parameter Estimation Methodology for the Analysis of Aeroheating and Thermal Protection System Experimental Data

Milad Mahzari[1]
Georgia Institute of Technology, Atlanta, GA, 30332

Ioana Cozmuta[2]
ERC Inc., Moffett Field, CA 94035, USA

Ian G. Clark[3] and Robert D. Braun[4]
Georgia Institute of Technology, Atlanta, GA, 30332

There are substantial uncertainties in the computational models currently used to predict the heating environment of a spacecraft and the Thermal Protection System (TPS) material response during Mars entry. Flight data will help with a better quantification and possible reduction of such uncertainties as well as with the improvement of the current computational tools. The Mars Science Laboratory (MSL) entry, Descent and Landing Instrumentation (MEDLI) suite will provide a comprehensive set of flight data. The Inverse Parameter Estimation (IPE) methodology presented in the current paper targets the reconstruction of the boundary conditions experienced by the spacecraft during the entry in the Mars atmosphere, in particular the heating to which the TPS is exposed. To investigate the feasibility of the IPE method, arcjet test conditions relevant to MSL entry environments are selected. The Nominal Analysis is performed first to examine the quality of the experimental data and to compare to the nominal model predictions. Next, a Monte Carlo study is performed to provide a hierarchy for the model input parameters based on their overall contribution to the measurement uncertainty. A Sensitivity Analysis is then performed where the correlation between the different input parameters is investigated to determine whether they can be simultaneously estimated. Finally, an IPE code is developed and tested on the Arcjet dataset. This code uses in depth temperature information and recession data to back calculate heating and material properties. Solution uniqueness, existence and stability are discussed in detail and are being identified as the main challenges of the inverse analysis.

Nomenclature

C_H	=	FIAT heat transfer coefficient = $\rho_e u_e c_h$
Cp	=	Specific heat
f	=	Scaling factor
G	=	Physical model
J	=	Sensitivity matrix
M	=	Number of measurements
N	=	Number of input parameters
P	=	Vector of input parameters
S	=	Sum of square of errors (objective function)

[1] Graduate Research Assistant, Guggenheim School of Aerospace Engineering, AIAA Student Member.
[2] Senior Research Scientist, Reacting Flows Branch, AIAA Member.
[3] Visiting Assistant Professor, Guggenheim School of Aerospace Engineering, AIAA Member.
[4] David and Andrew Lewis Associate Professor of Space Technology, Daniel Guggenheim School of Aerospace Engineering, AIAA Fellow.

$\mathbf{T}$ = Vector of direct problem outputs (FIAT predictions)
X = Sensitivity coefficient
$\mathbf{Y}$ = Vector of measurements
Δ = Normalized 2σ uncertainty = $(2\sigma / x_{nom})$
ε = Emissivity, Error
κ = Thermal conductivity
μ = Damping parameter
ρ = Density
$\mathbf{\Omega}$ = Diagonal matrix

Subscripts
c = char property
i = index of input parameter
k = time index of thermocouple temperature prediction
v = virgin property

Superscripts
k = Levenberg-Marquardt iteration number
T = Transpose of a matrix

I. Introduction

The Thermal Protection System (TPS) is a critical component of most Earth and planetary missions and is responsible for protecting the spacecraft against entry aeroheating. When spacecraft travel to other planets for surface missions or when they return to Earth upon the completion of their missions, they are required to enter a planet's atmosphere at very high velocities and safely land on the surface. During entry, the interaction between the spacecraft and the planet's atmosphere will dissipate more than 99% of the entry system's initial kinetic energy, mostly in the form of heat. The heatshield will keep the aeroshell interior safe from these extreme environments. Since the TPS is critical to mission success, the aeroheating environment and TPS material response have to be modeled accurately. However, there are substantial uncertainties associated with the analytical models that are currently used for predicting aeroheating and TPS response. These uncertainties have a significant effect on the TPS material selection and total mass, and therefore limit our ability to design more capable and robust Entry, Descent and Landing (EDL) systems.

Flight data can help scientists reduce these uncertainties to improve or validate the current computational tools. During the past few decades, there have been numerous entry missions that were equipped with instruments to collect aeroheating and TPS performance data. These missions were primarily in support of the Apollo program.[1] Many lessons have been learned from these efforts, but some of the returned dataset have either not been critically evaluated or they were not sufficient for code validation. Moreover, a majority of these instrumented missions have occurred in the Earth atmosphere. However, Mars has been and will continue to be a frequent destination in recent space exploration efforts. Mars Pathfinder was the only mission equipped with forebody TPS instruments.[2] The need for Martian flight data is further justified since the experimental facilities on Earth are not capable of fully recreating Mars flight conditions. Mars Science Laboratory (MSL), scheduled to launch in the fall of 2011, is instrumented with aerodynamic and aeroheating sensors. The MSL aeroshell is a 4.5-meter diameter spherically-blunted 70-degree half-angle cone with a triconic afterbody.[3] MSL's heatshield is made of an ablative material called Phenolic Impregnated Carbon Ablators (PICA). A uniform PICA thickness of 1.25 in is used. MSL Entry, Descent, and Landing instrumentation (MEDLI)[4] includes in-depth thermocouples and isotherm sensors. The MEDLI dataset will provide the first non-Earth entry aeroheating data since the Pathfinder mission, and will provide more flight data than all of the previous Mars missions combined.

The flight data acquired by MEDLI will help answer some of the fundamental questions related to aeroheating and TPS performance (material response) while also addressing the uncertainties associated with the current tools. A systematic post-flight data analysis strategy is required to maximize the benefits obtained from the MEDLI data. The main goal of this research is to develop relatively general and easy to modify methodologies and tools to analyze MEDLI aeroheating and TPS flight data to address the existing uncertainties, improve the current computational models and provide recommendations for future mission instrumentations. The suite of tools and methodologies we

refer to as the Inverse Parameter Estimation (IPE) method will reconstruct, using the data provided by the MEDLI instrumentation the surface heating and TPS material properties. The IPE method is based on the minimization of an objective function containing both calculated and measured temperature by adjusting several predefined parameters until a solution is obtained.

The objective of this paper is to describe the development of the IPE methodology and its validation using a selected set of MSL Arc jet test data. Section II describes the primary uncertainties associated with the current computational models used for predicting MSL heating and TPS performance. Section III provides an overview of the MEDLI instrumentation suite with emphasis on the aeroheating subsystem, MEDLI Integrated Sensor Plugs (MISP). Section IV describes the arcjet test set used to validate the IPE method. The IPE method consists of four steps (Section V): Nominal Analysis, Uncertainty Analysis, Sensitivity Analysis and Inverse Analysis. These steps help identify the input parameters with significant contributions to the overall uncertainty, which parameters can be estimated, what range of data needs to be considered, and how the estimation process should be implemented. Section VI discusses how the developed methodology is applied to the selected MSL arcjet test dataset to estimate the desired heating and TPS parameters. Finally, the main challenges faced in the inverse parameter estimation process are discussed in detail.

II. Current Modeling Uncertainties

Modeling uncertainties are divided into two subgroups: uncertainties due to aerothermal modeling, and uncertainties due to TPS material response modeling. The current section will discuss such uncertainties from the perspective of Mars entry with emphasis on carbon/resin based ablators as a primary material for the heatshield. Most of these uncertainties however are also relevant for other planetary atmospheres.

In a recent paper, Wright et al.[5] reviewed the current status of aerothermal analysis for Mars entry missions and the uncertainties associated with the current models. In a carbon dioxide environment, the two primary uncertainties in forebody heating prediction are turbulence and surface reactions. Prior to MSL, all Mars missions flew mostly laminar trajectories; heating augmentation due to turbulent flow not being a major concern. The MSL vehicle however is larger than any previous Mars missions. Future human missions to Mars will require even larger entry vehicles. For such large vehicles, transition to turbulence happens early on in the trajectory and turbulent heating becomes a dominant factor. Significant uncertainties exist in the current knowledge and modeling of turbulent flow especially as related to the onset of turbulence, i.e. transition. Turbulent heating may also be augmented due to the roughness effects generated by the ablation of the TPS material. Figure 1 (right) compares MSL centerline heating for laminar flow using different turbulence models. It is evident that turbulent flow greatly increases heating when compared to the laminar heating predictions.

Surface catalysis, the process in which the surface of the TPS material mediates recombination of the species from the boundary layer with additional heat deposition to the surface, is also an important source of uncertainty. The models currently used for characterizing such chemical reactions have not been validated and there are still large unknowns in these models especially related to the reaction rates. Usually catalytic effects are modeled using a conservative upper limit, that of supercatalytic wall. Figure 1 (left) shows the MSL centerline catalytic heating for an early MSL design trajectory as calculated using different catalysis models. It can be seen that the peak heat flux ranges from 47 W/cm^2 for the non-catalytic surface to 125 W/cm^2 for the supercatalytic surface (a factor of 3). Clearly, a better understanding of this phenomenon and a more accurate estimation of catalytic heating could reduce the current design margins which consequently could result in significant performance gains.

For TPS material response modeling, the primary uncertainty is the recession rate of the TPS material, especially in a dissociated shear flow environment. Such flow is normally seen in the leeside of the forebody heatshield. PICA recession is governed mainly by oxidation of the carbon char. Since the Martian atmosphere is mainly composed of carbon dioxide, there is significant uncertainty in the carbon oxidation modeling in a dissociated carbon dioxide atmosphere. The primary reason for this uncertainty is the lack of experimental capability to validate the ablation model. Currently, there is no U.S. ground facility capable of conducting a test with a high enthalpy dissociated carbon dioxide environment. Uncertainty in recession modeling impacts both the distribution of the energy terms in the surface energy balance as well as the in-depth material response, mainly the in-depth temperature profiles. One of the direct results of the MEDLI post flight analysis will be to compare measured in-depth temperature profiles with the model predictions and address such uncertainties. A second important component in modeling the behavior

of ablative materials is represented by the set of employed material properties for both virgin and char. Some of these thermal properties (char thermal conductivity, pyrolysis gas enthalpy, etc) are difficult to be measured accurately at high temperatures. MEDLI provided flight data could provide better information about the material properties exhibited by the ablative material in flight environments.

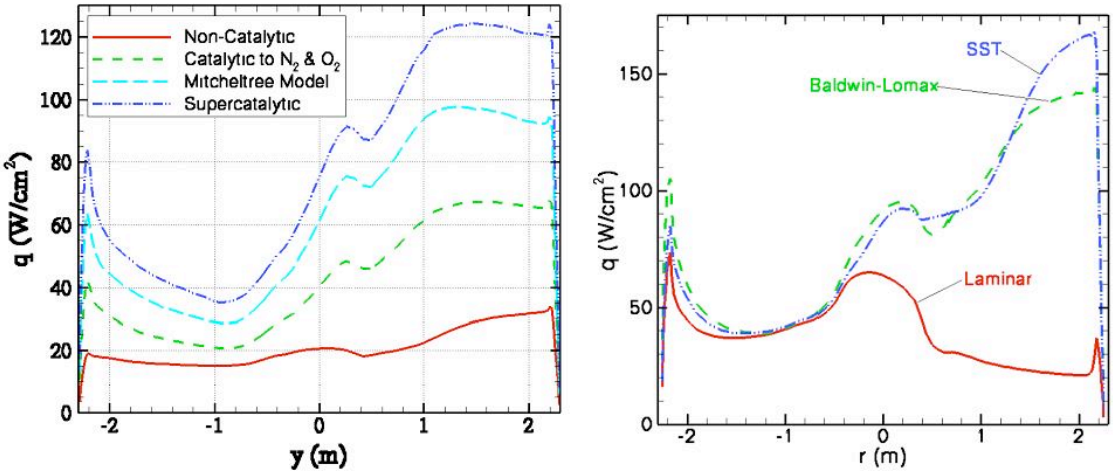

Figure 1. Uncertainties in MSL centerline heating for an early MSL design trajectory for various catalytic heating models (left) and respective turbulent heating models (right) [5]

III. MEDLI

MEDLI consists of seven pressure ports and seven integrated sensor plugs at different locations on the MSL heatshield. The suite consists of three subsystems: MEDLI Integrated Sensor Plug (MISP) temperature/isotherm sensors, MEDLI Entry Atmospheric Data System (MEADS) pressure sensors, and Sensor Support Electronics (SSE). The sensors are installed into the PICA plugs that are flush-mounted to the flight heatshield. The MISP locations (Figure 2, T labels) cover a broad range of heat flux environments, while the MEADS locations (Figure 2, P labels) are concentrated in the higher pressure and lower heat flux region near the stagnation point and the nose region. The data from the MISP sensors are the focus of this research. Table 1 summarizes the design environments for the MISP sensor locations.

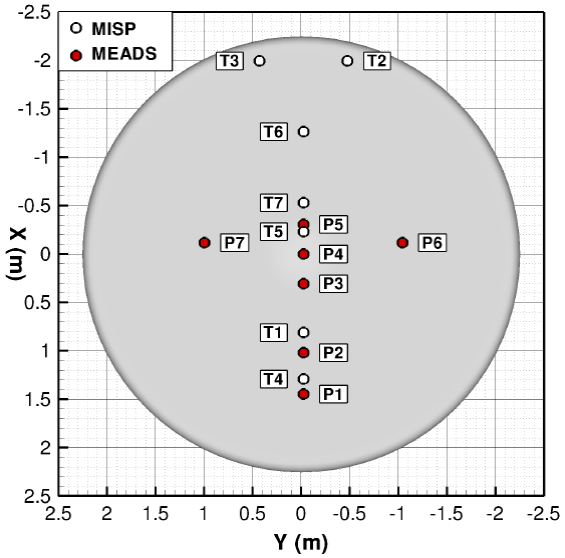

Table 1. MISP plugs design aerothermal environment [3]

Location	Peak q_w (W/cm^2)	Peak τ_w (Pa)	Peak p_w (atm)	Q_w (J/cm^2)
T1	56	8	0.371	2345
T2/T3	189	376	0.267	5168
T4	52	7	0.370	2092
T5	107	124	0.265	3637
T6	184	285	0.264	5028
T7	118	101	0.48	3711

Figure 2. MEDLI sensor locations on the MSL heatshield[3]. The location of the pressure sensors (MEADS) is indicated by the P labels while that of the temperature/isotherm sensors (MISP) is indicated by the T labels.

Each MISP plug is 33 mm in diameter with a total depth of 20.3 mm, and contains four type-K U-shaped thermocouples.[4] The thermocouples are approximately at 2.54, 5.08, 10.16, 15.24 mm from the surface of the plug. The top two thermocouples are intended primarily for heating reconstruction, while the two deeper thermocouples are primarily intended for material property reconstruction. The science measurement range requirement for each thermocouple is 100 to 1300 K with an accuracy of ± 2.2 K or 2.0% below 273 K and ± 1.1 K or 0.4% above 273 K. The top thermocouple is sampled at 8 Hz while the deeper thermocouples are sampled at either 1 or 2 *Hz* depending on the location. Each MISP plug also contains an isotherm sensor named Hollow aErothermal Ablation and Temperature (HEAT).[6] The HEAT sensor measures the temporal progression of 700 °C isotherm through the TPS. The sensor elements are conductive and as the char layer-virgin material interface advances these elements become shorter and the voltage output decreases. The measurement range is 0 to 13 mm with an accuracy of ± 0.5 mm. The HEAT sensor is sampled at 8 Hz. Figure 3 shows a completed HEAT sensor and MISP plug.

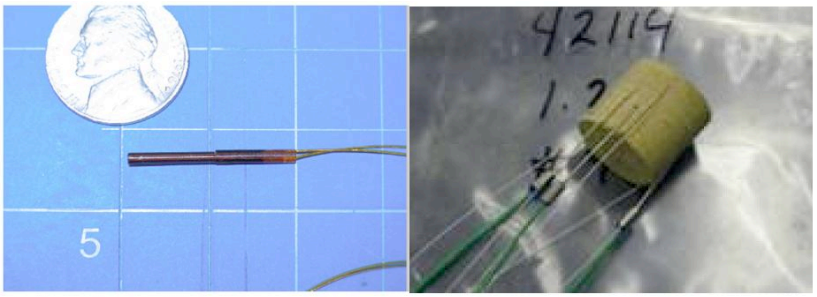

Figure 3. Completed HEAT sensor (left) and MISP plug (right) [6]

IV. Arcjet Test Selection

Arcjets are the main ground facilities employed for the testing and qualification of TPS materials and spacecraft heatshields. The heating environment for a given mission can be approximately simulated in arcjets and by placing an instrumented TPS material sample in the generated flow, one can study the TPS ablation and its in-depth performance. Multiple tests were carried out at the NASA Ames Research Center Arcjet Complex in the support of MSL heatshield development and qualification. For the purpose of the current study, arcjet test conditions (series AHF 271) relevant to the MISP operating environments are selected. Stagnation tests were performed using 4 inch Iso-q pucks to assess the in-depth thermal response of PICA in the heating environment of MSL. Thirty four arcjet runs were performed at 10 different aeroheating conditions. Most of the samples were instrumented with five thermocouples at varying depths.

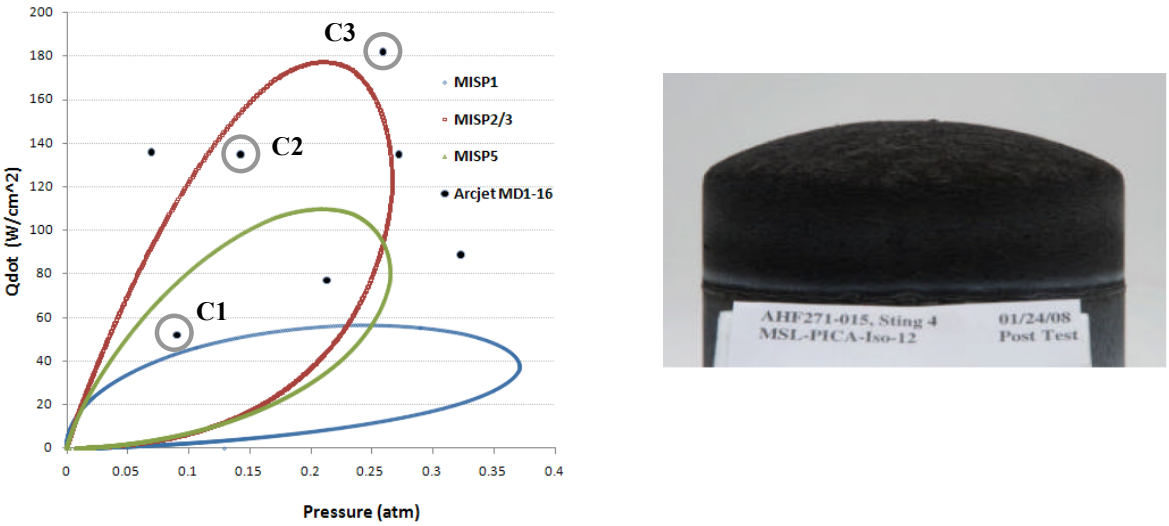

Figure 4. Left: Arcjet test conditions and envelope of predicted MISP heating environment. Right: Image of a post-test AHF 271 Iso-q sample.

The test conditions and the envelope representative to the MISP flight heating environment are plotted in Figure 4. These environments were derived using a supercatalytic and fully turbulent assumption, and including 3σ trajectory uncertainty. Details in terms of heat flux, pressure, test duration and corresponding ablation model temperature and recession error prediction for the three arcjet test conditions selected to represent the MISP heating environment (circles in the Figure 4) are given in Table 2. The model error represents the % errors of the difference between the measurements and the computational model predictions.

Table 2. Heating environment and corresponding model error for the three selected arcjet tests in Figure 4

Condition	Run #	Heat Flux (W/cm2)	Pressure (atm)	Test Duration (s)	% Temp Error	% Recession Error
C1	271-06	52	0.09	120	8-16%	17%
C2	271-12	135	0.142	50	7%	1.5%
C3	271-15	182	0.259	35	4%	3%

While thermal conduction problems are usually easy and more accurate to model, ablation physics is a more complex phenomenon. The various approximations employed by the computational codes to model ablation may end up being inaccurate for some heating regimes introducing significant deviations from the actual physics happening. Since inverse parameter estimation methods usually wrap around such ablation models, the estimation of the model input parameters is as accurate as the physics and chemistry represented by the model. In other words, an inverse analysis may be only as good as the direct analysis upon which it builds. The current study utilizes the Fully Implicit Ablation and Thermal Response Program (FIAT) to model the TPS material performance and sizing (Reference 7). FIAT is an implicit ablation and thermal response program for simulation of one-dimensional transient thermal energy transport in a multilayer stack of isotropic materials that can ablate from a front surface and decompose in-depth. FIAT is developed by scientists at the NASA Ames Research Center and is a standard tool in the aerospace industry today for the thermal sizing and analysis of spacecraft heatshields. The equations solved in the FIAT code are the internal energy balance, internal decomposition, internal mass balance and surface energy balance equations. The B' tables employed by the FIAT code are derived under the assumption of thermochemical equilibrium at the surface. This assumption is usually valid at high heating conditions. At lower heating conditions, finite-rate chemistry dominates and thus recession tends to be overestimated by the FIAT code. To investigate the FIAT model error for the three selected arcjet test cases listed in Table 2, the thermocouple temperature history is plotted with the FIAT predictions of in-depth temperature. These plots are shown in Figure 5 for both the lowest and highest heating arcjet test cases.

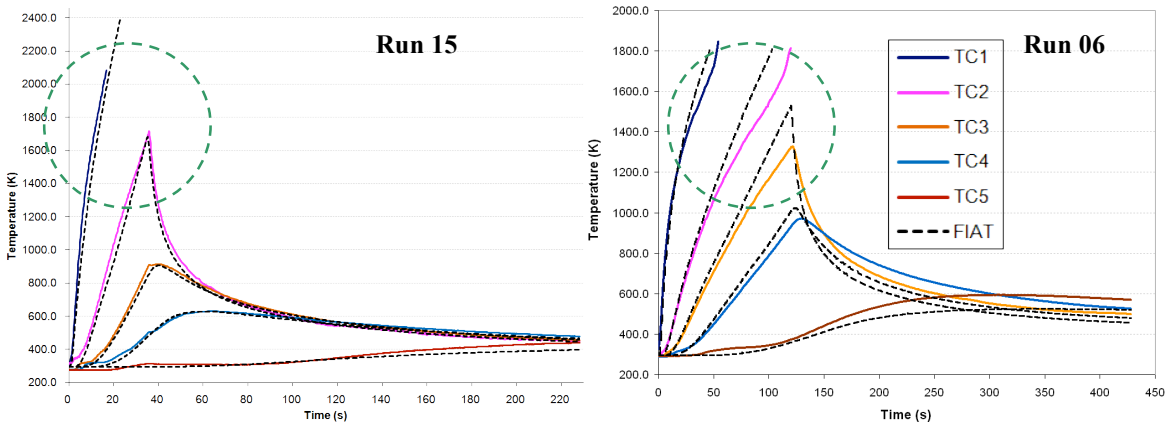

Figure 5. FIAT Low model error for high heating case (left) and high model error for low heating case (right)

Indeed, Figure 5 confirms that the model error (in terms of both temperature and recession) for the lower heating case (C1) is larger than that for the higher heating case (C2) with C3 intermediate. To ensure that FIAT is operated under the domain of validity of its assumptions, C3 with the lowest model error is selected for the IPE exercise. This arcjet test corresponds to a stagnation heat rate of 182 W/cm^2 and a stagnation pressure of 0.259 atm. The duration of the test is 35 seconds after which and the sample was removed from the arcjet chamber and left at ambient temperature for cool down. Post-test measurement revealed the recession to be 5.2 mm.

V. Methodology

An inverse parameter estimation methodology has been developed here for a more comprehensive analysis of aeroheating and TPS experimental data. The development of this methodology is motivated by future analysis of the MISP flight data; however, in lieu of actual MISP data, the arcjet test case described above is used to test the methodology and investigate its feasibility. This methodology needs to be general enough to be applied to other experimental data with minimal modifications or additions. The purpose of this methodology is to systematically estimate target design parameters from experimental data. Typically in most engineering problems, a theoretical model is developed to represent the physics of the problem, design parameters are selected and then the system's response is calculated. This is called a direct problem as simplified in Equation 1.

$$\mathbf{T} = \mathrm{G}[\mathbf{P}] \tag{1}$$

where T is the system's response (outputs), P is the design input parameters, and G is the physical model. In the direct problem G and P are known and the goal is to find T. Conversely, experimental analysis relies on the knowledge of the measurements of the system's response (T) and the physical model (G) and the goal is to estimate the input parameters (P). This is called an inverse problem. Inverse problems are solved using inverse parameter estimation methods. In the simplest sense, these methods are based on the minimization of an objective function containing both the measured system's response and the response predicted by the physical model. The parameters that minimize this objective function are considered the solution of the inverse problem. IPE methods iterate on input parameters until the closest possible match between measurements and calculations is achieved. However, the above equation is the simplest case possible, a perfect scenario, where the physical model perfectly captures the physics of the problem and the measured response exactly represents the true response of the system. In this case, the estimated parameters will be the true system parameters. Real life applications however need to account for various sources of uncertainty, being a random noise, a statistical dispersion, a measurement error or a bias. Thus, Equation 2 given below is a more realistic representation of the problem:

$$\mathbf{Y} = \mathbf{T} + \left(\varepsilon_{random} + \varepsilon_{bias}\right) = \mathrm{G}[\mathbf{P}_{true}] + \varepsilon_{model} \tag{2}$$

where Y is the measurements of the system's response. As shown on the left hand side of the equation, in reality the measurements are not exactly the same as a system's true response due to measurement errors. The errors could be either random, which lead to noise in the measurements or they could be in the form of a bias in the measurements. An example of a bias error is the thermal lag of a thermocouple meaning that there is a lag between the temperature that the thermocouple is showing and the actual temperature of the material. Additionally, we can have measurement errors due to instrument malfunctions. The right hand side of the equation shows that in reality the physical model is not always perfect. Theoretical models are our best effort in modeling a physical phenomenon and therefore do not always represent the physics exactly. This difference is called model error. If fewer approximations are used in developing the physical model the total model error would be lower. In current ablative TPS modeling, there are many approximations used due to the complicated nature of the problem. Therefore, as we have seen in the arc jet test conditions discussed earlier, the model error could be significant

Measurement and model errors pose several challenges to inverse problems. Now, one cannot be certain that the estimated parameters are the true system parameters. The estimation process could converge to a solution that is not the true solution. It is important to identify these errors and try to minimize them. When they cannot be avoided, effort should be made to perform the estimation process in a way that the results are not affected by these errors. Another issue in inverse problems is the possible non-uniqueness of the solution. Different parameter combinations could result in similar system responses leading the estimation process to converge to more than one solution making the simultaneous estimation of multiple parameters not possible. The existence of the above-mentioned complexities can make the estimation process very unstable. Avoiding this situation is a major motivation for developing a comprehensive methodology.

Before approaching a problem using the IPE methods, one needs to perform preparatory steps to ensure that estimation process is done correctly and to maximize the benefits from the results. What is the quality of the experimental data? How much random and bias error does it have? What range of the data can be trusted? How does the current nominal response compare to the experimental data? How significant is the model error? What are the parameters we want to know? Which parameters are the most significant contributors to the uncertainty? What is the

sensitivity of the outputs to the input parameters? How correlated are the parameters with each other? Which parameters can be estimated simultaneously? The methodology developed in this paper provides an answer to these questions and proposes guidelines on how to conduct the parameter estimation via four steps: Nominal Analysis, Uncertainty Analysis, Sensitivity Analysis, and Inverse Analysis. More details on these steps and how they are applied to the test problem on hand are given in the following sections.

A. Nominal Analysis

This step requires the examination of the experimental data, review of the current modeling approach, and comparison of the measurements to the predicted nominal response. The examination of the experimental data targets the identification of possible sources of measurement errors. Measurement errors are usually minimized by smoothing the data and removing bias errors. Also, data anomalies such as non-physical features or instrumentation malfunctions have to be identified. These data anomalies may be removed by simple interpolation methods; however, sometimes these anomalies can not be fixed and the data should be considered untrustworthy and disregarded. Such examination of data quality is done for the arcjet test problem and the details are discussed in "Implementation & Results" section.

The examination of the current modeling approach and the predicted nominal response implies that one needs to understand how the direct problem is currently being done before embarking on the inverse analysis. Since the physical model is the central piece of both the direct and the inverse analysis, it is important that the model as well as its assumptions and limitations are well understood. This information directly feeds into understanding the model error, i.e. the accuracy of the physical model in representing the problem on hand. Discussion of the details of ablative TPS response modeling is available in literature and is not the focus of this paper. As discussed before, the arc jet condition selected for the IPE study corresponds to a very small model error, i.e. falling in a regime where the material response model FIAT is known to be reasonably accurate. The application of this step to the selected arcjet test dataset is explained in "Implementation & Results" section.

B. Uncertainty Analysis

The uncertainty analysis is performed to identify what design parameters need to be estimated by the IPE method and what range of measurements must be used in the estimation process. This process defines a hierarchy of the aerothermal variables and material properties based on the largest uncertainty contribution to the in-depth temperature predictions. This step also provides great insight into the direct problem and expected qualitative trends, which is a prerequisite for any inverse analysis. The approach employed to accomplish these goals is probabilistic and is accomplished with Monte Carlo simulations.

Aerothermal and TPS designs and analyses are typically deterministic. A probabilistic TPS design to demonstrate the use of Monte Carlo techniques in determining TPS margins was first discussed by Dec and Mitcheltree[8] for the proposed Mars Sample Return Earth Entry Vehicle. However, only a small number of input parameters were studied. Extensive studies performed by Bose et al.[9,10] also showed the great potential of Monte Carlo simulation as a technique to predict the uncertainties in aerothermal environments. Chen et al.[11] demonstrated a general Monte Carlo technique for establishing appropriate TPS thickness margins and for performing sensitivity studies. They applied this technique to the TPS design for several space entry vehicles. Building on this work, Sepka and Wright[12] developed a Monte Carlo analysis software tool and applied it to the MSL aeroshell TPS design. The tool helped them determine the parameters that have the greatest influence on the MSL bondline temperature.

All these studies have demonstrated the utility of a probabilistic methodology to quantify the uncertainty levels, and rank sources of input uncertainties. This study uses the same technique and tool as Reference 12 to perform the Monte Carlo study. The software tool used to perform Monte Carlo simulations is called McFIAT[12] which is a PERL-scripted code for use with FIAT. These simulations are done for a range of uncertainties in aerothermal variables and material properties. Gaussian distributions are used for these input parameters. Ten thousand runs are performed to ensure statistical accuracy. The nominal values used in this study for the input parameters are the current design values of for PICA material properties and CFD predictions of the arcjet heating parameters. The material property uncertainties are primarily determined via expert judgments based on the experience in predicting material performance during experimental testing.[13] The input aerothermal variables' uncertainties are based on previous works done on the probabilistic analysis of the uncertainties in the computational models used to predict the heating environment. Table 3 shows the normalized 2σ uncertainty values (Δ) for both aerothermal and material input parameters used in this Monte Carlo study.

Table 3. Normalized 2σ uncertainties used in the Monte Carlo study for input parameters

Material Input Parameter	Δ	Aerothermal Input Parameter	Δ
Virgin density	0.05	Surface pressure	0.15
Char density	correlated	Blowing reduction in C_H	0.20
Virgin specific heat	0.05	Heat transfer coefficient, C_H	0.15
Char specific heat	0.10		
Virgin conductivity	0.15		
Char conductivity	0.15		
Virgin emissivity	0.03		
Char emissivity	0.05		
Pyrolysis gas enthalpy	0.20		
Resin decomposition rate	0.20		
Char recession rate	0.04		
Initial material temperature	0.05		

One modification has been made to McFIAT code for this study. In McFIAT, the uncertainty values are independently defined and the code does not take into account correlations between the different parameters. Furthermore, the code checks to make sure that the random value generated for char density is always less than the value generated for virgin density. In doing so, the code creates artificial skewness in the char density distribution. Figure 6a shows the virgin and char density scaling factors as generated by a Monte Carlo run with the original McFIAT and the skewness can be clearly seen. A skewed distribution for an input parameter results in skewed distributions in output parameters which invalidates the normal distribution assumption used in the analysis of the results. Since these two material properties are not independent and are correlated, correlations were implemented in McFIAT for these parameters. Many tests have been done to measure virgin and char densities of PICA samples. Using the results of these tests one can develop a probabilistic equation relating the two. Figure 6b shows such a study that was done at NASA Ames Research Center. A linear equation with uncertainty bars was derived based on the experimental data. Now, one can generate random values of virgin density and calculate the char density from the derived equation. This capability is added to McFIAT. Figure 6c shows the virgin and char density scaling factors as generated by a Monte Carlo run with the modified version of McFIAT and no skewness can be seen in distributions.

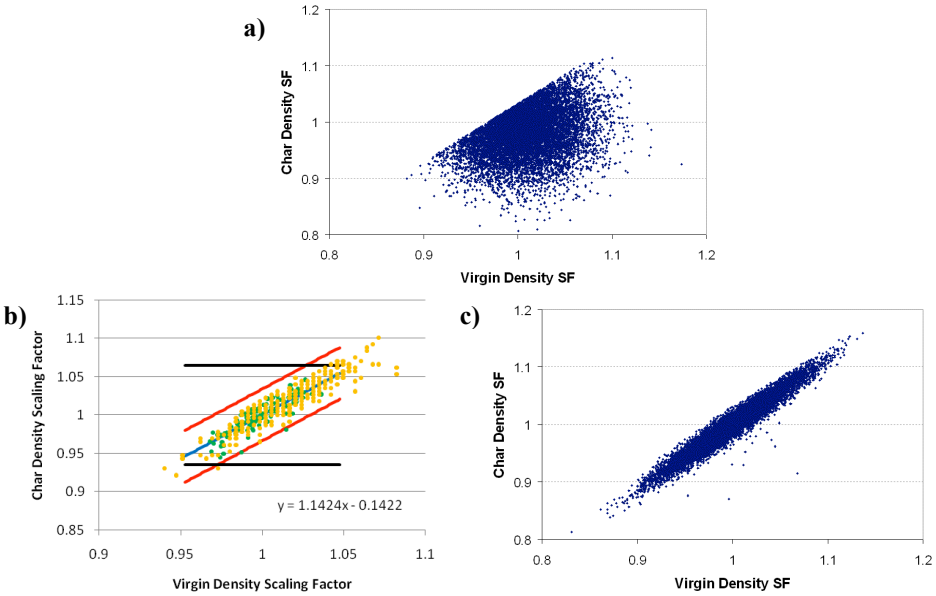

Figure 6. Addition of correlation to McFIAT removes the skewness problem

The Monte Carlo post-processing is traditionally done using linear regression analysis by calculating the relative contribution of each input's variability to the overall output's variability[12]. The input-output correlation coefficients are first computed. In this study the outputs of interest are time-dependent temperature predictions at the thermocouple locations and the final recession. The square of the correlation coefficient is interpreted as the fractional contribution to the uncertainty in the output due to the uncertainty in the input parameter. Traditionally a pie chart is used to illustrate the percent contribution of the input parameters for a certain output. This illustration is useful when the outputs are single-valued numbers such as final bondline temperature or final recession. This has been the case in the Monte Carlo work done in literature. However, a thermocouple measures the temperature over time and it is important to show the time evolution of these uncertainty contributions. Therefore, in this work for the first time this regression analysis is done in a time-dependent manner. To illustrate time dependent results, area charts (sand charts) are used instead of pie charts. Each vertical slice of the area chart represents a pie chart. These charts help us determine what parameters are the most important parameters and what time range is most sensitive to those parameters.

The results of the Monte Carlo analysis for the selected arcjet case are presented in the "Results & Implementation" section. It should be noted that even though this analysis is a powerful tool for identifying the parameters with the highest contribution, any Monte Carlo analysis is only as good as the code used to solve the direct problem. Therefore, if there are any deficiencies in FIAT's ability to fully capture the physics of the problem in certain conditions, such deficiencies will affect the reliability of the Monte Carlo analysis. Some problems with FIAT have been already discussed, so the reader should remember that the Monte Carlo results presented in this paper are only as good as FIAT's accuracy.

C. Sensitivity Analysis

The Monte Carlo Analysis only identifies the most important parameters but it provides no information on the magnitude of the effect that the input parameters have on the output parameters, or the correlation between the input parameters. These two pieces of information have important implications on the inverse analysis. In inverse analysis a parameter can be easily estimated if it has large effect on the measured outputs and if it is not correlated with other inputs. If two parameters are correlated they have similar effects on the measured outputs, and it becomes very difficult to estimate these parameters independently. Therefore a FIAT-based sensitivity analysis needs to be performed before the inverse analysis. This analysis will tell us what parameters can be estimated simultaneously. The sensitivity analysis is done by calculating sensitivity coefficients of the outputs to input parameters (partials of the outputs to the inputs). These partials are approximated using central difference as shown in equation 3.

$$X_{i,k} = \frac{\partial T_k}{\partial P_i} = \frac{T_k(P_i + h) - T_k(P_i - h)}{2h} \tag{3}$$

In the above equation "h" is a small change in the input parameter, T is the output of interest (in this case predicted thermocouple measurements) and P is an input parameter. The calculated sensitivity coefficients are plotted as a function of time for all the parameters to investigate the correlation between the parameters. The results of the Sensitivity Analysis for the selected arcjet case are given in the "Implementation & Results" section.

D. Inverse Analysis

All the previous steps provide crucial information for the last step which is Inverse analysis. Using all the information obtained, in Inverse Analysis we plan and execute an estimation process. At the core of Inverse Analysis are the IPE methods. Before defining the details of this step, a review of some past IPE work in related fields is presented.

1. Review of Past Work

IPE techniques have been used widely for a broad range of applications. These methods are utilized to estimate physical parameters characterizing a model from collected observations. As a result, these methods have been used in variety of fields where direct measurement of physical parameters is either impossible or difficult. During Mars EDL, entry vehicles go through a quick sequence of events in harsh conditions making the direct measurement of parameters difficult. Therefore, IPE methods have been utilized to reconstruct EDL trajectory parameters and atmospheric conditions for most Mars missions. References 14 and 15 discuss the current methods for trajectory and

atmosphere reconstruction of Mars entry vehicles. For the sake of brevity, this section discusses only the past IPE work in the heat transfer field. An important application of the IPE methods in the heat transfer field is the estimation of material thermal properties and surface heat flux. Normally, it is difficult to measure these parameters directly due to lack of reliable instruments, harsh working conditions and the high cost of experimental set up. The reader can refer to Reference 16 for a more detailed discussion of Past IPE work in the heat transfer field.

Estimation of the thermal properties of solid materials has been widely studied. In 1966 Beck[17] developed a methodology to estimate thermal conductivity and specific heat of nickel given transient temperature measurements using least-square minimization methods. He also discussed the design of experiments for which the thermal properties of a material can be accurately determined. Sawaf and Ozisik[18] estimated linearly temperature-dependent thermal conductivity components and specific heat of an orthotropic solid using the Levenberg-Marquardt iterative method. Haung and Yan[19] estimated thermal conductivity and specific heat using the conjugate gradient method. Dantas and Orlande[20] employed a function estimation approach to determine temperature-dependent thermophysical properties using the conjugate gradient method. Dowding[21] used parameter estimation techniques to estimate thermal properties of a carbon-carbon composite by combining experiments in a sequential manner. Garcia[22] used genetic algorithms to estimate thermophysical properties of composite materials.

The estimation of properties for ablative materials is more complicated than regular solid materials since ablative materials pyrolyze and recede. Little IPE work has been done with ablative materials. Oliveira and Orlande[23] used the conjugate gradient method with adjoint problem to identify the heat flux at the surface of an ablating material from simulated measurements of temperature and the position of the ablating surface. Kanevce[24] et al. estimated the thermal properties of an ablative material using the Levenberg-Marquardt method. Silva and Orlande[25] estimated an ablator's thermal properties using a combination of the Levenberg-Marquardt method and the sequential parameter estimation technique. Molavi et al.[16] utilized the Levenberg-Marquardt method to estimate temperature-dependent thermal conductivity and specific heat of the noncharring ablator carbon-carbon using simulated measurements. They used the CMA code for modeling the ablative material response. In summary, the estimation of properties of solid materials has been extensively studied using different IPE methods. Application of IPE methods to estimate the ablative material properties is relatively new. Different gradient based least-square optimization methods have been used for ablative materials with some success. The current results look promising even though more work is required in this field.

2. IPE Code

This study applies the methods and lessons learned from past work to the problem on hand. First an IPE code needs to be developed for this problem. For the arcjet test problem, we are trying to estimate certain material properties and heating parameters from the arcjet data. As mentioned before, the IPE methods estimate these parameters by trying to match the predicted outputs with the measurements. Therefore, an important part of the IPE code is the code representing the direct problem (the physical model). Like previous steps FIAT is used to model the direct problem of ablative material response. The diagram below shows the structure of the IPE code developed.

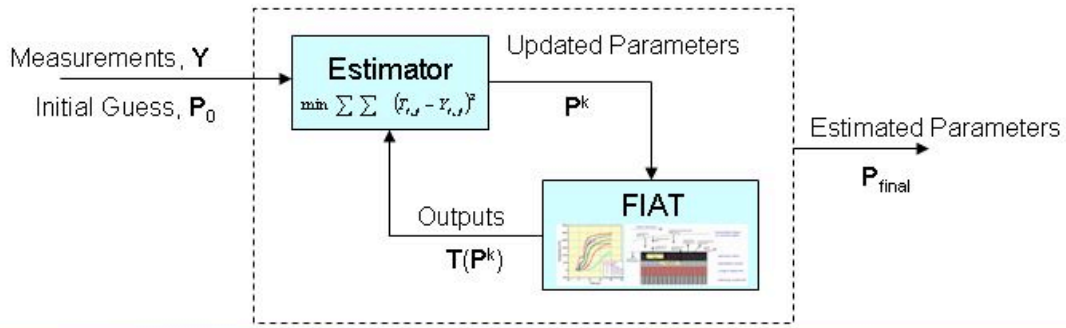

Figure 7. Structure of the IPE code

In the simplest sense, the IPE code is an optimizer which requires the solution of the direct problem at different steps. Therefore, the code is written to wrap FIAT meaning that it is able to create FIAT input files based on the current values of the input parameters and parse the FIAT output files and get the outputs of interest. In this case the input parameters are material properties and heating parameters and the outputs of interest are time-dependent in-

depth temperature predictions at the five thermocouple locations. The estimator is an IPE algorithm. In this problem, a least square minimization algorithm is employed to perform the parameter estimation. Most of the past work for ablative materials has used gradient-based optimization methods such as Levenberg-Marquardt method or the conjugate gradient method. For this test problem we use the Levenberg-Marquardt method because it has shown success in dealing with these kinds of problems. The code is written mainly in MATLAB while two FORTRAN programs are used to wrap FIAT. The code operation starts with an initial guess for the parameters, then FIAT input files are generated and FIAT is run. The output files are parsed and the outputs of interest are returned to the estimator. The IPE algorithm updates the parameters to minimize the difference between predicted outputs and measurements. This process is repeated until convergence is achieved.

The heating and material input parameters used in the IPE code are not the actual dimensional values, but they are non-dimensional scaling factors with respect to the current nominal values. This choice of parameters makes the coding simpler and is also useful because one can easily see how much the parameters change from the original nominal values by the estimation process. Also, there are many heating and material input parameters that go in FIAT; however not all these parameters are major contributors. Therefore, the code is written only for a subset of the input parameters. This subset was identified through the Monte Carlo analysis described earlier. The detailed results for the Monte Carlo analysis are given in the later sections. The top contributors are identified as heat transfer coefficient (heating), density, virgin and char specific heat and thermal conductivity, and char emissivity. The parameters vector is shown the equation below where *f* denotes scaling factors:

$$\mathbf{P} = [f_{C_H}, f_{Cp_v}, f_{Cp_c}, f_{\rho}, f_{\boldsymbol{K}_v}, f_{\boldsymbol{K}_c}, f_{\boldsymbol{\varepsilon}_c}] \tag{4}$$

The code is written so that the user has control over what parameters to estimate. One can have the code estimate all the above parameters, or a smaller subset of them. Furthermore, the code has the capability of generating simulated data. Simulated data are useful in code validation and debugging. Also simulated data show a scenario where the data and model is perfect because the data is created by the model. Therefore, simulated data can be used to discuss some limitations of inverse analysis that have nothing to do with the quality of the data or model.

3. Levenberg-Marquardt Method

The Levenberg-Marquardt method is an iterative method for solving nonlinear least squares problems of parameter estimation. This method estimates the parameters by minimizing the sum of squares of the errors between the measured temperatures and the calculated temperatures as predicted by the code used to model the direct problem. This method is mainly based on the calculation of a sensitivity matrix at every iteration. The sensitivity coefficients in this matrix are partial derivatives of the predicted temperatures with respect to estimation parameters. At each iteration, the parameters are updated based on these sensitivity coefficients and other information. This technique was derived as a method that would tend to the Gauss method in the neighborhood of the minimum and would tend to the steepest descent method in the neighborhood of the initial guess. This is done using a damping parameter which reduces oscillations and instabilities due to the ill-conditioned nature of inverse heat transfer problems in the region around the initial guess.

The details of the Levenberg-Marquardt computational algorithm[26] are summarized below. In the algorithm below, **P** is the vector containing the parameters that need to be estimated (defined by Eq.4); **Y** is the vector containing the measured temperatures at different times and from different sensors (in this problem, thermocouples 1-5 measurements); and **T** is a vector containing the corresponding temperatures as predicted by the code used to model the direct problem (in this problem, material temperature as predicted by FIAT at thermocouple locations). The algorithm shown below describes the steps at iteration *k*:

1) Solve the direct problem with the current estimate of parameters $\mathbf{P}^k$ to obtain the predicted temperatures $\mathbf{T}(\mathbf{P}^k)$.
2) Compute the sum of square of errors $S(\mathbf{P}^k)$ using the equation below. Superscript T is transpose.

$$S(\mathbf{P}^k) = \left[\mathbf{Y} - \mathbf{T}(\mathbf{P}^k)\right]^T \left[\mathbf{Y} - \mathbf{T}(\mathbf{P}^k)\right] \tag{5}$$

3) Compute the sensitivity matrix **J** using the following equation. The sensitivity coefficients are calculated using central difference approximations.

$$\mathbf{J} = \begin{bmatrix} \frac{\partial T_1}{\partial P_1} & \frac{\partial T_1}{\partial P_2} & \cdots & \frac{\partial T_1}{\partial P_N} \\ \frac{\partial T_2}{\partial P_1} & \frac{\partial T_2}{\partial P_2} & \cdots & \frac{\partial T_2}{\partial P_1} \\ \vdots & \vdots & & \vdots \\ \frac{\partial T_M}{\partial P_1} & \frac{\partial T_M}{\partial P_2} & \cdots & \frac{\partial T_M}{\partial P_N} \end{bmatrix} \tag{6}$$

4) Solve the following linear system of equations to find $\Delta\mathbf{P}^k$

$$\left[\left(\mathbf{J}^k\right)^T \mathbf{J}^k + \mu^k I\right] \Delta\mathbf{P}^k = \left(\mathbf{J}^k\right)^T \left[\mathbf{Y} - \mathbf{T}\left(\mathbf{P}^k\right)\right] \tag{7}$$

5) Compute the new estimate $\mathbf{P}^{k+1}$ as

$$\mathbf{P}^{k+1} = \mathbf{P}^k + \Delta\mathbf{P}^k \tag{8}$$

6) Solve the direct problem with the new estimate of parameters $\mathbf{P}^{k+1}$ to obtain the predicted temperatures $\mathbf{T}\left(\mathbf{P}^{k+1}\right)$. Compute the new sum of squares of the errors $S\left(\mathbf{P}^{k+1}\right)$.

7) If $S\left(\mathbf{P}^{k+1}\right) \geq S\left(\mathbf{P}^k\right)$, replace μ^k by $10\mu^k$ and return to step 4.

8) If $S\left(\mathbf{P}^{k+1}\right) < S\left(\mathbf{P}^k\right)$, accept the new estimate $\mathbf{P}^{k+1}$ and replace μ^k by $0.1\mu^k$.

9) Check the stopping criteria. If the stopping criterion is satisfied, stop the iterative procedure; otherwise replace *k* by *k+1* and return to step 3.

VI. Implementation & Results

In the previous section, the four steps of the proposed methodology for the TPS experimental data analysis were explained and the goals for each step were discussed. In this section, the developed methodology will be tested using the selected arcjet test data. We will show the benefits gained from each step of the methodology and discuss the major limitations and challenges faced in an inverse analysis. This practice gives us valuable information and experience on how to analyze the future MISP data and what are the areas that require more investigation.

A. Nominal Analysis

The main goal of this step is to examine the quality of the data. As discussed before, random and bias errors could cause instability and inaccuracy in the estimation process, therefore it is important to remove these errors before performing the inverse analysis. The arcjet data are in form of time-dependent thermocouple measurements. Some of the problems with the quality of this data are discussed here. First, the thermocouple measurements have random noise that could be easily smoothed out. In addition, there are other data anomalies that are shown in the figure below. One example is the sudden increase ("bump") in the beginning of thermocouple data shown in Figure 8a. This is seen in most arcjet data and is believed to be due to some unexplained exothermic reaction. Further problems with the data are shown and circled in Figure 8b. This anomaly is probably due to a sensor malfunction. There is no way for FIAT to model these features. Another problem with the data is that the thermocouples start at different temperatures as shown in Figure 8a. This could be due to both varying in-depth temperature of material and sensor malfunctions. In FIAT, only one initial temperature can be defined for a material layer, therefore we have to make sure the data for the different thermocouples start at the same temperature.

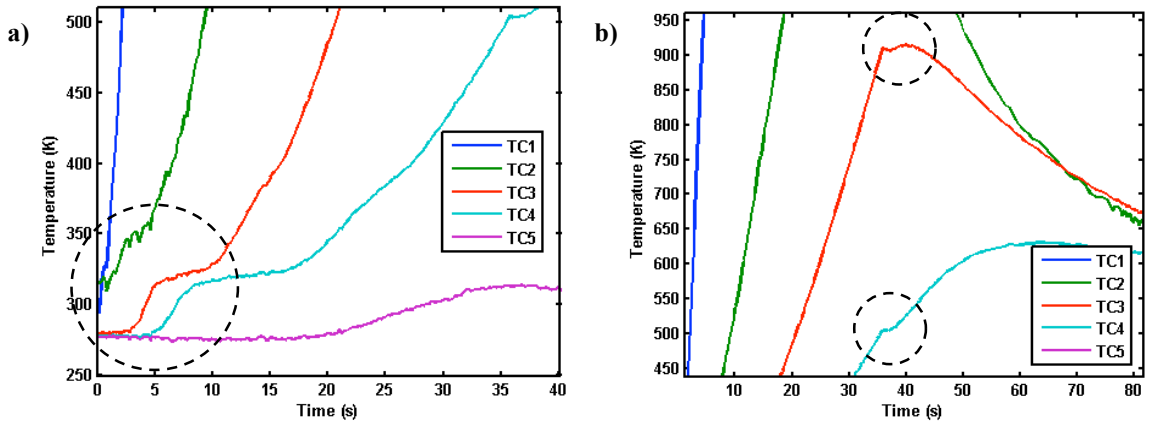

Figure 8. Data anomalies and non-physical features in arcjet thermocouple data

As mentioned before, there is no way for FIAT to model these data anomalies; therefore they need to be corrected for before the inverse analysis. The random noise in the data is reduced with a 5-point moving average data smoother in MATLAB. Figure 9a shows the original data and the smoothed version for one of the thermocouples. The initial bump in the thermocouple data is removed by using MATLAB's cubic spline data interpolation. The beginning of the thermocouple data is made asymptotic to remove the sudden bump. Figure 9b shows how this is done for one of the thermocouples. The data anomalies shown in Figure 8b are also corrected using the same spline data interpolation function. Figure 9c shows how this is done for one of the thermocouples. The fact that the thermocouples' starting temperatures are different is corrected by considering only the temperature rise. In other words, all the thermocouple measurements are shifted to the same initial temperature, 294 K (same number used in FIAT simulations). This is shown in figure 9d.

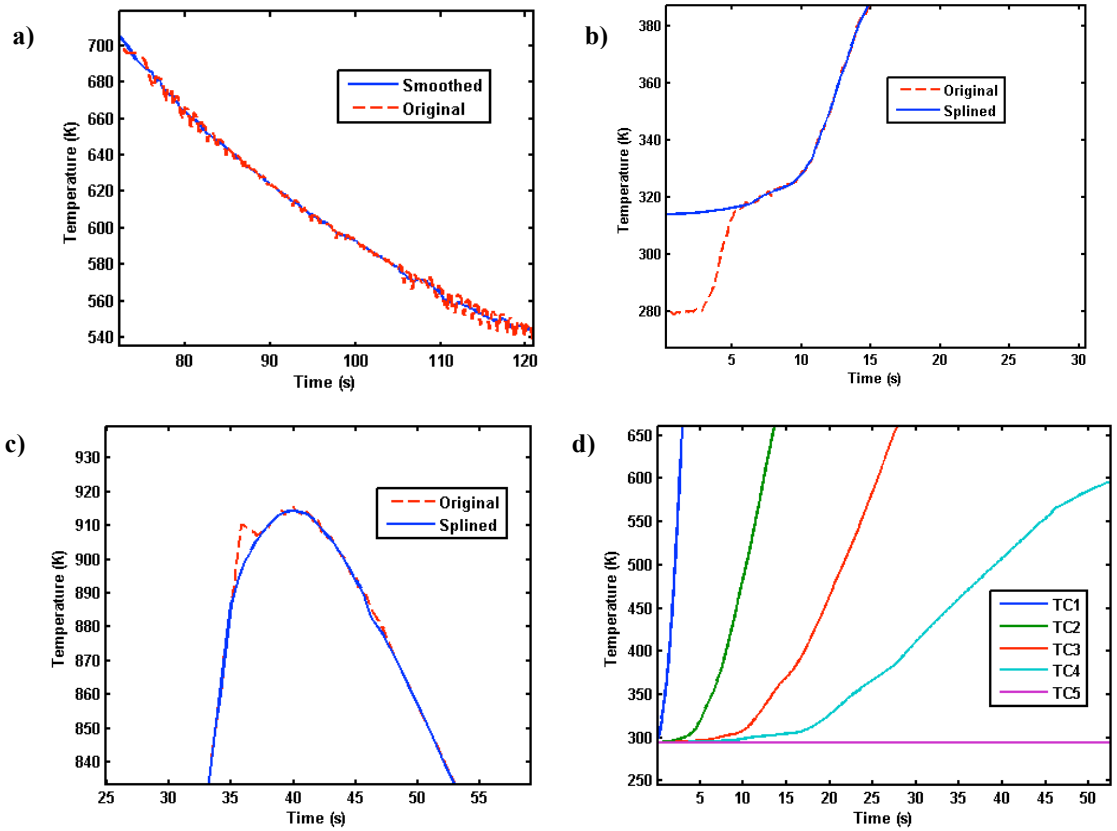

Figure 9. Measures taken to improve the quality of the experimental data

Another goal of this step is to compare the experimental data to the nominal TPS response as predicted by the physical model, FIAT. Figure 10a shows the thermocouple measured temperature compared to the nominal FIAT temperature predictions at thermocouple locations. In the inverse analysis we try to match these two sets by changing the input parameters; therefore, it is important to compare them beforehand. This comparison also helps us identify where the physical model has obvious deficiencies. Overall, there is a good agreement between the two sets. There are some discrepancies and data anomalies that are corrected as explained before. The data match very well for TC1-3 for most of the early part of the test. However, we can see that the difference increases for the later times in the test and also for TC4-5 data. The reason for this trend is 2D effects. FIAT is a 1D heat transfer code and does not account for in-plane heat transfer. In reality, there is heat transfer in both in-depth and in-plane directions. For heatshields or large arcjet coupons, the in-plane heat transfer is insignificant; therefore 1D heat transfer is a good assumption. However, this test was performed with a small 4 inch coupon and the 2D effects are important. Also FIAT models only surface heating. In the arcjet environment the gas going around the coupon transfers provides some lateral heating to the coupon in addition to the surface heating. If the coupon is small the lateral heating reaches the thermocouples faster. Therefore, the lateral heating becomes significant for a small coupon, deeper thermocouples and for the longer test durations. This is the case for this arcjet run. Therefore, the data from deeper thermocouples and later times is not as useful because of the 2D effects that FIAT can not model. This is an important finding for planning the inverse analysis.

Figure 10b also shows the nominal material response as predicted by FIAT. In this figure, the recession, char and virgin depths are plotted as a function of time. On the same plot the depth of the five thermocouples is shown. This plot is important because one could see what the state of the material is at any given time at any thermocouple locations. This helps us in explaining the trends and results seen throughout the Monte Carlo and Sensitivity analyses.

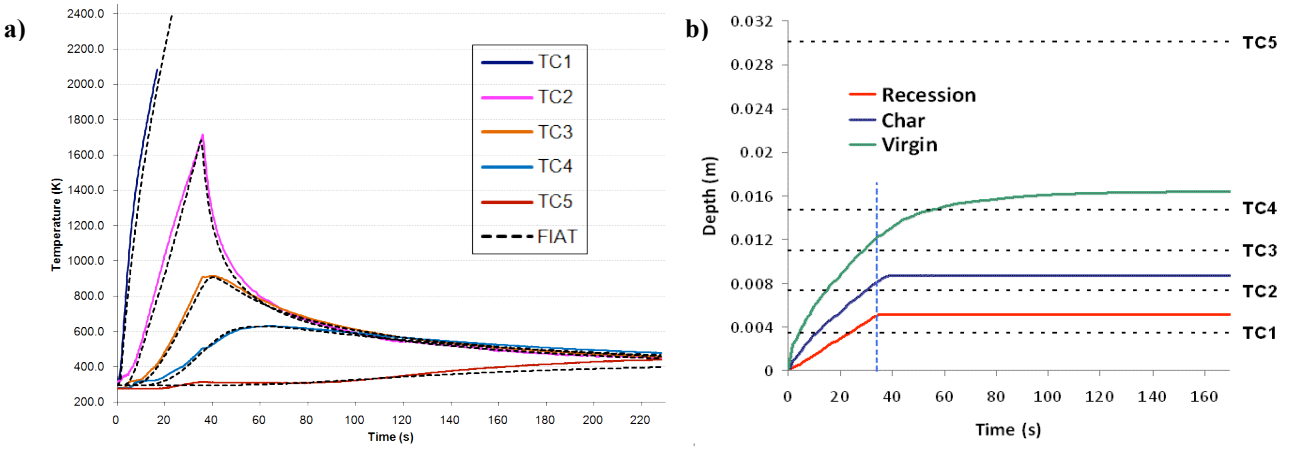

Figure 10. Comparison of the experimental data to the nominal TPS response

B. Uncertainty Analysis

The main purpose of the uncertainty analysis is to identify the parameters that contribute the most to the uncertainty of the predicted thermocouple measurements. This exercise tells us what parameters should be of most interest for the inverse analysis. The input parameters are heating and material parameters, while the outputs are the time-dependent predicted temperatures at five the thermocouple locations and the final recession. Since the predicted temperatures are time-dependent, the results can not be shown with traditional pie-charts; therefore, one area chart is employed for each thermocouple. However, the final recession is not time-dependent and a simple bar chart is employed. Figure 11 shows the percent contribution of the input parameters to these outputs. Not all the input parameters are major contributors; therefore, only the top contributors are labeled. Thermocouple 1 is the closest to the surface and burns out once the surface recession reaches its depth. For this reason, the results for TC1 are shown for a shorter time than the other thermocouples.

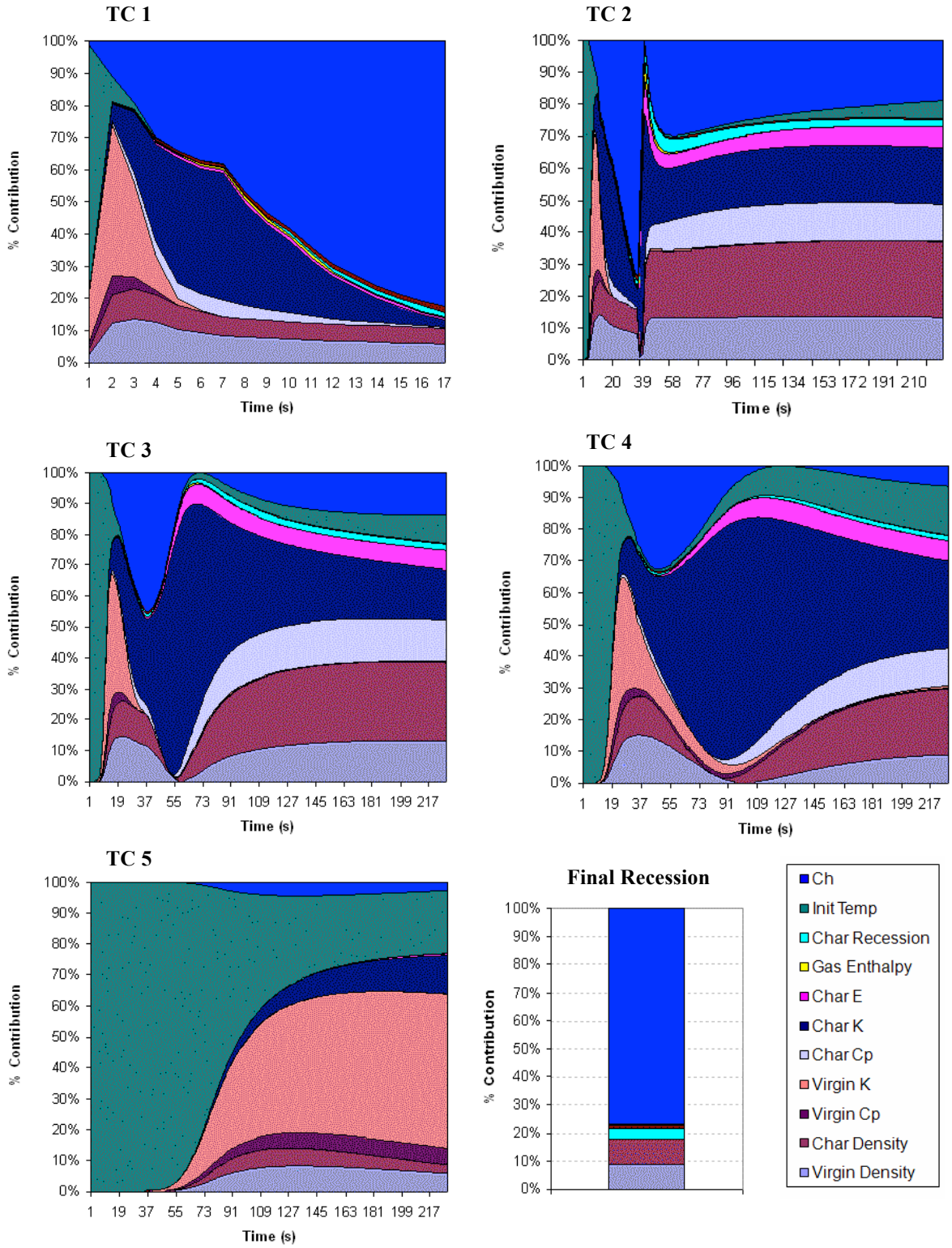

Figure 11. Percent contribution of the input parameters to the predicted measurements uncertainty

When interpreting these plots it is important to know the state of the material at each thermocouple as a function of time. Different input parameters become important whether the thermocouple is in the char zone, pyrolysis zone or virgin zone. Figure 10b (the depth plot) provides this information. However, the Monte Carlo analysis also gives us the capability to put uncertainty bars on the recession, char and virgin depths. The figure below shows recession,

char and virgin depths as a function of time with 2σ uncertainty. On the same plot we can see the location of the thermocouples.

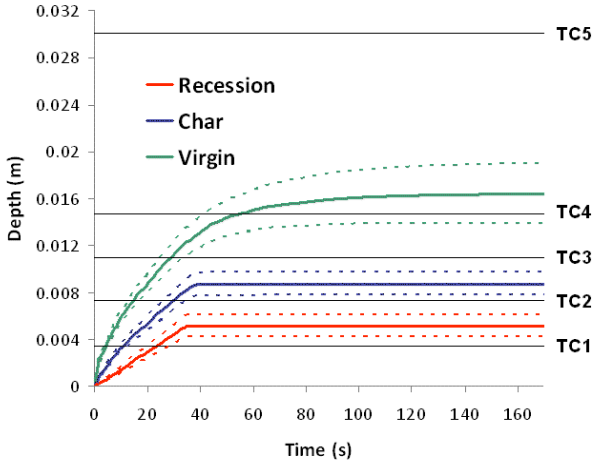

Figure 12. Time-dependent recession, char and virgin depths with 2σ uncertainty

Looking at the above plot, we can now interpret the area charts given in Figure 11. The first thing to notice is that the same trend shifted in time can be seen in all the thermocouples. This is indicative of the time that it takes for the heat to transfer in the material. For all the thermocouples, we can see that the initial material temperature is the top contributor in the beginning. This parameter is not important for inverse analysis, because we can easily take the material initial temperature to be the same as thermocouple initial reading. As the time increases, we can see that the virgin properties become important. At this time the material is mainly virgin and the heat transfer is governed mainly by these parameters. In particular we can see that virgin conductivity and density are the top contributors. These two parameters control the thermal diffusivity and the material's heat absorption.

We can also see that as time increases the heat transfer coefficient's importance increases. The longer it goes, the TPS material senses the effects of surface heating more and therefore the heating parameters become more important. For the same reason we can see char emissivity becoming more important. This is due to the fact that the char emissivity controls the surface re-radiation. Therefore, higher char emissivity results in lower effective input surface heating. Next we can see the char properties, specifically char thermal conductivity and specific heat becoming important. At this point the material is charring from the top and pyrolyzing in the middle. This creates char and pyrolysis zones in the material in addition to the virgin zone. The pyrolysis zone material properties depend on both virgin and char properties which explain why the char properties become more important. To point out the connection between the material state and the Monte Carlo results more clearly, we can look at Figure 12 for TC4. We can see that TC4 enters the pyrolysis zone some time between 40-55 s. Now if we look at the area chart for TC4 in Figure 11, we can see that char thermal conductivity's contribution becomes significant around 40 s and increases.

Comparing between different thermocouples we can see that the heating parameters are most important for the thermocouples close to the surface while material properties are more important for the thermocouples deep in the material. For example, TC5, which is the deepest thermocouple, is almost entirely affected by material properties. Finally, looking at the bar chart for final recession we can see that it is mainly affected by heat transfer coefficient and density. This is important observation for inverse analysis. For example, if the experimental and theoretical recessions match well, it means that our current nominal values for the heat transfer coefficient and density are good estimates. Later, we use this observation in the inverse analysis.

Another interesting but non-intuitive observation is that the heat transfer coefficient's contribution increases as time increases but then suddenly goes to zero and then increases. To explain this behavior, we have to remember that the material sample was kept in the arcjet for 35 s and then it was removed to cool down for the rest of the run time. The higher the heat transfer coefficient the hotter the sample gets, and the faster it cools down. Therefore, for a low heat transfer coefficient the TC temperature goes up to some value and then drops slowly once it is removed. However, for a high heat transfer coefficient the TC temperature will go higher but then it would drop faster when it

comes out of arcjet. Therefore, one could conclude that there would be a crossing time where TC temperature is not affected by the heat transfer coefficient. This behavior can be easily seen in the Figure below. Figure 13 shows the different temperature profiles for TC3 when heat transfer coefficient is varied from -20% to +20% of the nominal value. We can see that all the profiles cross each other at about 70 s. Now looking at the area chart fro TC3 in Figure 11 we can see that the contribution of heat transfer coefficient drops to zero around the same time.

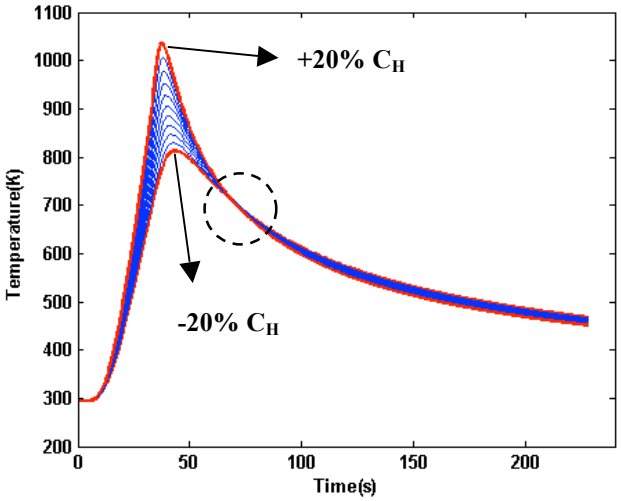

Figure 13. TC3 temperature profiles for varying heat transfer coefficients

A rather surprising observation is that pyrolysis gas enthalpy does not show up as a top contributor in the Monte Carlo plots. From physical intuition one would expect the gas enthalpy to be a major driver due to the amount of energy released through pyrolysis. Similar trends have been observed in other independent FIAT Monte Carlo studies. Currently, the authors have no explanation for this observation, but it is important to remember that the Monte Carlo analysis is only as accurate as FIAT. Therefore, if FIAT does not capture the importance of a parameter the Monte Carlo analysis won't either.

There are many other interesting observations that can be made from the generated area charts and the Monte Carlo analysis in general. However, for the purposes of the IPE work, the main conclusion from this analysis is the identification of the top contributors. We have already seen that some of the parameters are not major contributors and don't show up in the area charts. Based on the discussion above, we have narrowed down the parameters to the top seven uncertainty contributors. These parameters are: heat transfer coefficient, char conductivity, virgin conductivity, density, virgin specific heat, char specific heat and char emissivity. These are the parameters that we are most interested in and would want to have a good estimate of.

C. Sensitivity analysis

As discussed before, the knowledge of the correlation between the input parameters is crucial for the inverse analysis because most IPE algorithms are gradient-based and use sensitivity coefficients in order to update the parameters. If the magnitudes of these sensitivity coefficients are small or if they are correlated with each other, it could cause problems with solution stability and uniqueness of the inverse method. Therefore, the sensitivity coefficients are numerically calculated for this arcjet test problem. The figure below shows the sensitivity coefficients for the input parameters and for the five thermocouple locations. Only the top seven parameters identified by uncertainty analysis are shown here. These plots show partials of the outputs to the inputs, effectively showing how much the thermocouple temperatures change for 1% change in the input parameters (one at a time).

The first observation in Figure 14 is that the closer the thermocouple is to surface the more the magnitude of its temperature is affected by the input parameters. In other words the top thermocouples are most sensitive to change in parameters and therefore the most useful in estimating these parameters. We can see the magnitude of the change decay as we go deeper to the point where TC5 is barely affected by a small change in the inputs. In addition to the magnitude of the sensitivity coefficient plots, one needs to also investigate the shape of these plots and compare them among the different parameters. This is traditionally done in order to investigate correlation and linear

dependency between parameters[27]. If two parameters have similar profiles, they have a strong linear dependency. This means that they have similar effects on the outputs and an estimator would not be able to distinguish between their individual effects. Therefore, such parameters can not be estimated simultaneously.

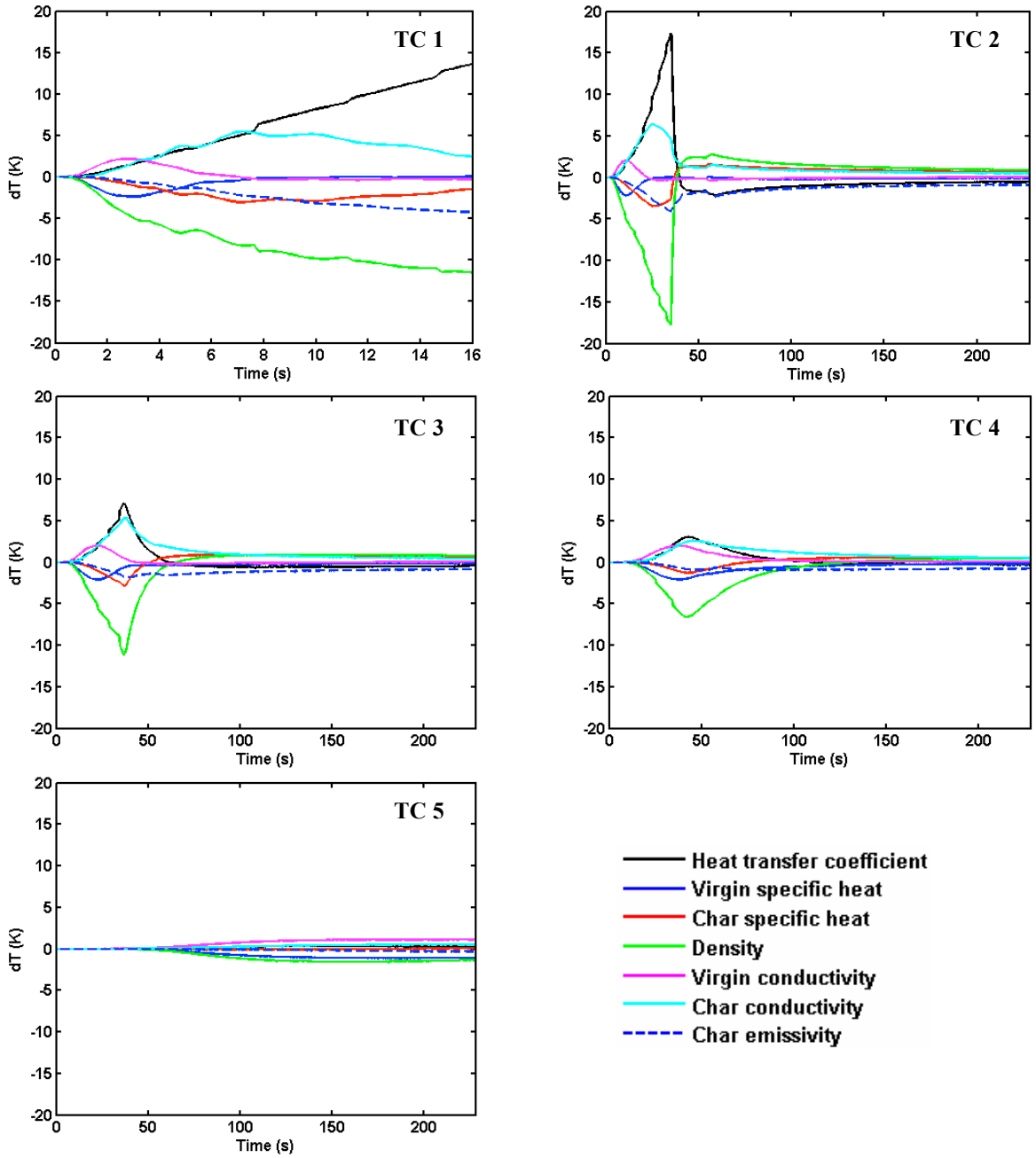

Figure 14. Sensitivity coefficient plots show correlation between different input parameters

Examining the shapes of the sensitivity coefficient profiles, at first we can see that the heat transfer coefficient and density have similar but inverse profiles. This means that increasing the heat transfer coefficient or decreasing density almost has the same effect on the material in-depth temperature. The same relationship can be seen between virgin conductivity and specific heat, and also between char conductivity and specific heat. The reason for this behavior is that the heat transfer through the material is mainly driven by thermal diffusivity which is directly proportional to the thermal conductivity and inversely proportional to the specific heat. In the FIAT governing equations, thermal conductivity always shows up as a quantity that is divided by the specific heat. Therefore increasing one or reducing the other will almost have the same effect. These parameters cannot be estimated

simultaneously. In conclusion, while the uncertainty analysis informs us of what parameters need to be estimated, the sensitivity analysis shows what parameters can be estimated simultaneously and independently.

D. Inverse Analysis

All the prerequisite information to plan a successful estimation process is now available. In this step, we perform the inverse analysis knowing the quality of the data, what parameters we want to estimate and what parameters we can estimate. However, we first need to verify the IPE code developed for this work. Next, the limitation of the code and the IPE problem in general is discussed. Finally a test problem is solved to show how the different steps of methodology come together.

1. Inverse Code Verification

The IPE code can be divided into two parts: the IPE algorithm (estimator) that calls FIAT in its solution process, and the wrapper script that performs FIAT Input/Output (I/O) operations. In the simplest sense the estimator is an optimizer. One needs to verify that the code converges to the true mathematical minimum to ensure that the objective function is globally minimized. In addition to mathematical verification, we need to show that the parameters estimated by the code are the parameters. We need to apply the code to a problem for which we know the true parameters and examine if the IPE code can converge to the true solution. The only case when we know the true parameters in advance is if we generate the data ourselves. Therefore, first we verify the code with simulated data.

Simulated data represents a perfect scenario meaning that the data is created by the same physical model that is used for the inverse analysis. In other words, there are no measurement errors or model errors. In such a case one would expect the code to converge to the same parameters that were used to generate the data. However, this is not always the case due to the limitations in inverse analysis. To show this, the following experiment is done. The current nominal parameters are used with FIAT to create the simulated data. Remember that the parameters in the code are scaling factors non-dimensionalized with respect to the nominal values. Therefore in this case the parameters used to generate the data are all 1's. Once data is generated, a random vector of parameters is used as the initial guess for the IPE code. If all goes well, the code should be able to recover the parameters back to the nominal values (all 1's). The code does that most of the time. However, if we want to estimate all the parameters simultaneously, the code sometimes converges to non-nominal parameters that have the same thermal response as the nominal parameters. This tells us that the inverse problem's solution is non-unique. In other words, different combinations of the parameters can result in similar thermal response (temperature profiles). However, the non-nominal parameters that the code converges to are not just random combinations. There is a pattern in them which can be physically explained according to the governing equations solved by FIAT. As an example, one of the solutions that the code converges to is given below:

$$\mathbf{P} = [f_{C_H}, f_{Cp_v}, f_{Cp_c}, f_\rho, f_{\boldsymbol{K}_v}, f_{\boldsymbol{K}_c}, f_{\boldsymbol{\varepsilon}_c}] = [1.05, 1.00, 1.00, 1.05, 1.05, 1.05, 1.05] \tag{9}$$

As a matter of fact if we replace 1.05 with any other number close to 1 (ex. 1.08), it results in the same material performance. At first this might seem odd, but we know that thermal response is governed by the in-depth energy balance and surface energy balance. The surface energy balance is composed of two terms: surface heating governed by Ch, subtracted from reradiation heating governed by emissivity. If these two parameters are equally perturbed from their nominal values they result in the same effective heating. Also, we showed before through the sensitivity analysis that density and Ch have opposite effects on the thermal response; therefore increasing both of them equally will cancel their individual effect and results in the same thermal response. Furthermore, the in-depth energy transfer is governed by thermal diffusivity which is equal to thermal conductivity divided by density and specific heat. If specific heat stays constant and we increase density and conductivity equally we get the same thermal diffusivity. Figure 15 shows the temperature profile for both the nominal parameters (i.e. true solution) and the non-nominal parameters.

The main conclusion here is that even with perfect data and perfect model, the simultaneous estimation of all the parameters is not possible due to the non-unique nature of the inverse problem. Of course, a simple way around this problem is not to estimate all of the parameters. If some of the parameters are not estimated and are set to their nominal values, the estimator forces the rest of the parameters to their nominal values in order to have the same thermal response. For example, in the case that was discussed above if one decides that density is known and only the other parameters are estimated, the IPE code converges to the true nominal solution.

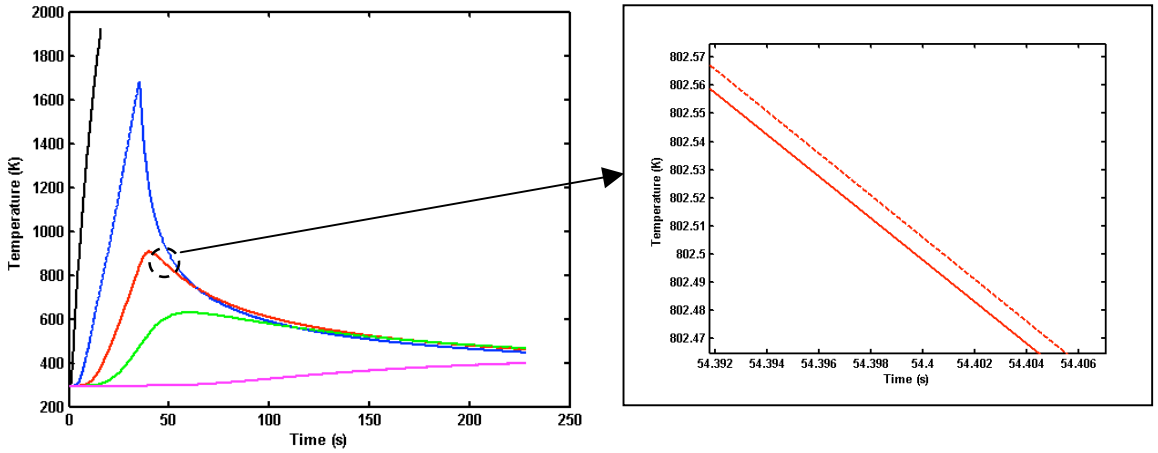

Figure 15. Non-nominal parameters result in the same thermal response as the nominal parameters

We also need to verify that the code is working properly with real experimental data. For an estimation problem with experimental data, there is no way to know the solution in advance and ensure that the code converges to the true solution. However, we can verify that the algorithm converges to the global minimum of the objective function. In the algorithm used here, the objective function is S, the sum of square of errors between the predicted temperatures and the thermocouple measurements. In order to verify that, first the code was used to estimate two parameters from arcjet experimental data. Then, an exhaustive search was done to find the true global minimum of S for the given parameters. In other words, FIAT is run for all the possible combinations of those two parameters (within reasonable limits), S is calculated for all those combinations, and the combination that makes S minimum is determined. Then we check if the IPE code converged to the true minimum. This process requires about four thousand FIAT runs and is very time consuming; however, it is important because it ensures us that the code is doing what it is supposed to. Here we estimate heat transfer coefficient and char conductivity with the IPE code, and then an exhaustive search is performed for these parameters. Figure 16 shows the result of the exhaustive search.

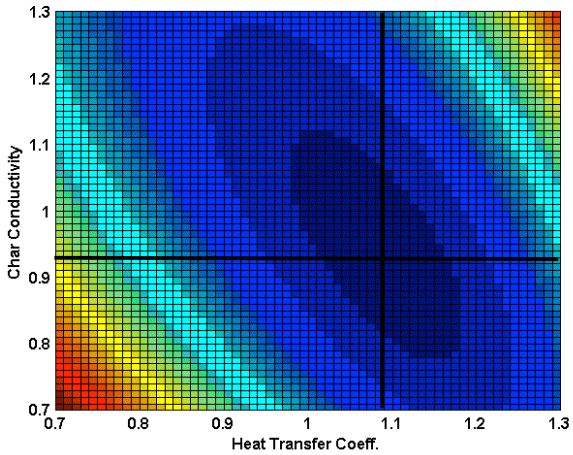

Figure 16. Exhaustive search shows that the IPE code converges to the true mathematical minimum

The IPE code converges to a heat transfer coefficient of 1.086 and char thermal conductivity of 0.928. Looking at Figure 16, we can see that the exhaustive search shows that the code has converged to the true mathematical minimum of the objective function.

2. Test problem

The developed IPE code for the arcjet problem has been verified. Now it is time to show how all the steps of the proposed methodology come together and how the final estimation process is planned according to what we have learned about the problem through the different analyses performed. Before that, we need to summarize some of the issues and challenges we have encountered in dealing with inverse problems and some suggested strategies on how

to deal with these challenges. The main issues could be categorized as solution existence, solution uniqueness and solution stability. As discussed before, in reality the experimental data have bias and random errors. Also the physical model used for the direct problem might not fully represent the physics of the problem. Because of these errors a direct relationship between parameters and the measurements might not exist. In other words, we can not find a set of parameters that can exactly match the experimental results. Therefore, most inverse problems do not have a solution in this exact sense. However, we can try to find the parameters that give us the best match with the experimental data. This raises many different questions such as what measure one should use to define the best match. Furthermore, the error in the experimental data translates to error in estimated parameters. If the measurement and model errors are large one can not be certain if the estimated parameters are good estimates of the true parameters. Another challenge faced in inverse problems is the non-unique nature of the solution. We showed earlier that even with perfect data and perfect model (i.e. no errors), different combinations of the parameters can result in the same thermal response. Therefore, an inverse problem could have more than one solution, and one can not be certain that the estimated parameters are the true parameters. Finally the last challenge faced in inverse problems is solution stability meaning that can we get the same solution under different circumstances. In other words, if we use different ranges of measurements or if we estimate different subsets of the parameters, do we get the same solution every time?

We need to use some strategies or guidelines in order to deal with these challenges. First the errors in the problem need to be minimized. The model error can be minimized by using high-fidelity physical models. For ablative TPS modeling, FIAT currently is the industry standard high-fidelity tool. However, there are many approximations in the way TPS modeling is done today which results in FIAT's inability to predict recession accurately for some heating regimes. There is definitely a need for higher fidelity models that capture the physics and chemistry of the problem more accurately. However, FIAT is the best available for now. In order to minimize model error, we have to ensure that the experiment is done for conditions where FIAT is reasonably accurate. In this work, this was done in the arcjet test selection. Another source of error is measurement error. This can be minimized by smoothing the data to remove random noise or by trying to correct for bias error. Also, if some data can not be trusted we need to disregard that part of the data. This could be due to simple sensor malfunctions or our inability to model a feature seen in data. We applied parts of this strategy in Nominal Analysis where we smoothed the data and made some corrections. Finally, in order to deal with the solution uniqueness and stability challenges we need to plan the estimation process carefully based on the results of the uncertainty and sensitivity analyses. We can not estimate all the parameters simultaneously. Therefore, based on the analyses we have done we have to select what parameters we want to estimate, decide what parameters we can estimate and what range of measurements we should use.

So for this arcjet problem, there are two questions to answer for the estimation process. What parameters we should estimate? What range of measurements we should use? To answer the first question, we have to examine the results of the uncertainty and sensitivity analyses. The uncertainty analysis helped us narrow the list of parameters down to the top seven uncertainty contributors. These are the parameters that cause the most uncertainty in our design and we need to have a good estimate of these parameters. However, the sensitivity analysis showed us that there is a strong linear dependency between thermal conductivity and specific heat, and between the heat transfer coefficient and density. This means that these parameters should not be estimated simultaneously. Another important fact is that the current nominal predicted recession matches very well with the experimental recession. From the uncertainty analysis, we showed that the final recession is affected mainly by heat transfer coefficient and density. Therefore, we can assume that our nominal values for these parameters are good estimates. Also density and specific heat are normally known with low uncertainty. Considering all these facts, we assume that density, specific heat and heat transfer coefficient are known and we estimate virgin and char thermal conductivity.

The second question to answer is what range of measurements we should use. TC4 and TC5 data are affected by the 2D effects and lateral heating because they are deeper in the material. There are some other data anomalies due to sensor malfunctions in the data for both these thermocouples. Such errors could cause problems in estimation and we can not trust these data. Furthermore, the thermocouples used for this test are only calibrated up to 1300 K and the data above this temperature can not be trusted as much. Considering these facts, we only use TC1-3 measurements up to 1300 K. Now that we know what parameters we want to estimate and what range of measurements need to be used, we apply the verified IPE code to this problem. The arcjet test experimental data are used. The current nominal values of the parameters are used as the initial guess. The estimation was performed and the code successfully converged to the solution below:

$$\mathbf{P} = [f_{K_v}, f_{K_c}] = [1.051, 1.060] \tag{10}$$

This means that the estimated values for the virgin and char conductivity are respectively 5.1% and 6.0% higher than the current nominal value for these parameters. Figure 17 shows the temperature profiles for the measurements, the initial guess (nominal), and the final estimated parameters (best match). This figure is zoomed-in to show the details.

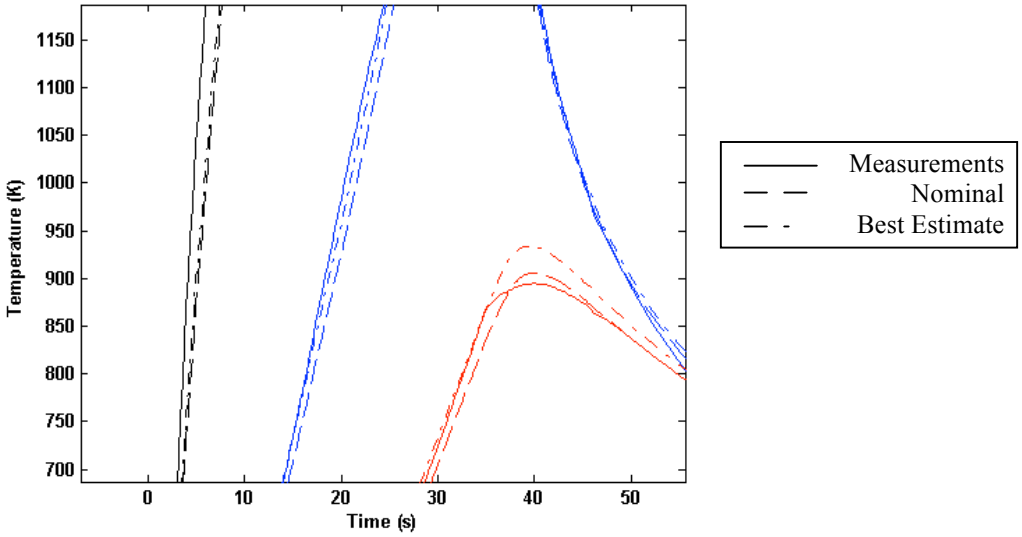

Figure 17. Through inverse estimation a better match with the experimental data is achieved

Looking at Figure 7, we can see that after the inverse estimation a better match with the experimental data is achieved. The estimated parameters are also within reasonable limits and the expected uncertainty associated with these parameters.

VII. Conclusions and Future Work

In this paper, a comprehensive inverse parameter estimation methodology for the reconstruction of surface heating and TPS material properties was developed. There are substantial uncertainties in our ability to predict the heating and the TPS material thermal response. The MEDLI instrumentation suite which will fly on the upcoming MSL mission was designed to provide valuable flight data for reducing these uncertainties and validating the current computational tools. A review of these uncertainties was presented, followed by an overview of the MEDLI instrumentation suite and the expected measurements. The main motivation for the development of this methodology is to maximize the benefits we get from the post-flight analysis of the MEDLI data. The developed inverse parameter estimation methodology was applied to an arcjet test dataset in order to investigate the feasibility of such approach. A discussion of the available arcjet data and the final selected test case was presented.

The proposed methodology is composed of four steps designed to provide the required prerequisite information for the inverse estimation of the heating parameters and material parameters. The first step was the Nominal Analysis where the quality of the experimental data was examined and a comparison to the current nominal predictions was presented. The second step was the Uncertainty Analysis where a Monte Carlo study was performed to identify the parameters that contribute the most to the measurement uncertainty, or in other words to identify the parameters that we want to estimate. For the selected arcjet test we determined that the heat transfer coefficient, char and virgin specific heat, thermal conductivity, density and char emissivity were the top contributors to the measurement uncertainty. The third step was the Sensitivity Analysis where the correlation between the different parameters was investigated in order to determine what parameters can be estimated simultaneously. In this step, we determined that there was strong correlation between the heat transfer coefficient and the density and between the specific heat and the thermal conductivity which meant that these parameters could not be estimated simultaneously. Finally, the last step was the Inverse Analysis where an inverse parameter estimation code was developed to

estimate heating and material parameters from the arcjet data. The developed code was verified and some of the limitations of the inverse approach were discussed. Solution existence, uniqueness and stability were identified as the main challenges faced in the inverse analysis. Some strategies were suggested in order to deal with these challenges. Finally, in order to show how the different steps of this methodology come together a test problem was solved to estimate the virgin and char thermal conductivity. The developed code successfully estimated these parameters by reducing the error between the arcjet thermocouple measurements and the temperatures predicted by the physical model, FIAT.

Future plans include a more detailed investigation of the challenges faced in the inverse analysis and possible strategies for dealing with them. This will also include a more detailed literature search of how IPE methods are used in other fields and how some of these issues are resolved. The current approach and the inverse tool developed for this problem is deterministic, so a future task would be to include stochastic capabilities. A stochastic tool would consider measurement uncertainties in its estimation methodology and therefore would be capable of estimating uncertainties in the estimated parameters. Next task will be to apply the tool to multiple available datasets such as other arcjet data, stardust and Mars Pathfinder data, and estimate heating environment and/or material properties for those datasets. This would be a useful practice in preparation for analyzing the future MISP data. Also, the reassessment of Pathfinder flight data could answer many fundamental questions related to Mars entry aeroheating and TPS performance. Next, a range of IPE methods could be implemented in the tool to compare the advantages and disadvantages of these different methods and identify the most appropriate one. Finally, the matured tool and methodology could be integrated with trajectory/aerodynamics reconstruction approaches in preparation for full MEDLI data analysis. By this time, a good knowledge will be gained about the problem and the challenges faced. Therefore, this knowledge can be used to develop methodology and guidelines for planning and designing future instrumentations in order to maximize the benefits of post-flight analysis.

Acknowledgments

The authors are grateful to Dr. Michael Wright (NASA Ames Research Center) for his help and guidance with this research. We are also grateful to Bernie Laub, Jose Santos and Todd White for their time to discuss some aspects of this work.

References

[1]Wright, M.J., Milos, F.S., and Tran, P., "Afterbody Aeroheating Flight Data for Planetary Probe Thermal Protection System Design," *Journal of Spacecraft and Rockets*, Vol. 43, No. 5, 2006, pp. 929-943.

[2]Milos, F., Chen, Y.-K., Congdon, W., and Thornton, J., "Mars Pathfinder Entry Temperature Data, Aerothermal Heating, and Heatshield Material Response," *Journal of Spacecraft and Rockets*, Vol. 36, No. 3, 1999, pp. 380– 391.

[3]Edquist, K.T., Dyakonov, A.A., Wright, M.J., and Tang, C.Y., "Aerothermodynamic Design of the Mars Science Laboratory Heatshield," *41st AIAA Thermophysics Conference*, June 2009, AIAA Paper No. 2009-4075.

[4]Gazaric, M., Wright, M., Little, A., Cheatwood, F. M., Herath, J., Munk, M., Novak, F., and Martinez, E., "Overview of the MEDLI Project," IEEE Paper 2008-1510, *IEEE Aerospace Conference*, Big Sky, Montana, March 2008.

[5]Wright, M., Chun, T., Edquist, K., Hollis, B., Krasa, P., and Campbell, C., "A Review of Aerothermal Modeling for Mars Entry Missions," *48th AIAA Aerospace Sciences Meeting*, January 2010, AIAA Paper 2010-443.

[6]Oishi, T., Martinez, E., Santos, J., "Development and Application of a TPS Ablation Sensor for Flight," *46th AIAA Aerospace Sciences Meeting*, January 2008 AIAA Paper 2008-1219.

[7]Chen, Y.K., and Milos, F.S., "Ablation and Thermal Response Program for Spacecraft Heatshield Analysis", *Journal of Spacecraft and Rockets*, Vol. 36, No. 3, 1999, pp. 475-483.

[8]Dec, J. A. and Mitcheltree, R. A., "Probabilistic Design of A Mars Sample Return Entry Vehicle Thermal Protection System," *40th AIAA Aerospace Sciences Meeting*, January 2002, AIAA Paper 2002-0910.

[9]Bose, D., Wright, M.J., and Gokcen, T., "Uncertainty and Sensitivity Analysis of Thermochemical Modeling for Titan Atmospheric Entry," *37th AIAA Thermophysics Conference*, July 2004, AIAA paper 2004-2455.

[10]Wright, M.J., Bose, D., and Chen, Y.-K., "Probabilistic Modeling of Aerothermal and Thermal Protection Material Response Uncertainties," *AIAA Journal,* Vol. 45, No. 2, 2007, pp. 399-410.

[11]Chen, YK., Squire, T., Laub, B., and Wright, M., "Monte Carlo Analysis for Spacecraft Thermal Protection System Design," 9th *AIAA/ASME Joint Thermophysics and Heat Transfer Conference*, June, 2006 AIAA Paper 2006-2951.

[12]Sepka, S., Wright, M., "A Monte Carlo Approach to FIAT Uncertainties- Improvements and Applications for MSL," *41st AIAA Thermophysics Conference*, June 2009, AIAA Paper 2009-4243.

[13]*NASA Internal Technical Document*, "CEV Thermal Protection System (TPS) Margin Management Plan," C-TPSA-A-DOC-7005.

[14]Christian, J.A., Verges, A.M., and Braun, R.D., "Statistical Reconstruction of Mars Entry, Descent, and Landing Trajectories and Atmospheric Profiles," *AIAA SPACE Conference and Exposition*, September 2007, AIAA Paper 2007-6192.

[15]Dutta, S., and Braun, R.D., "Mars Entry, Descent, and Landing Trajectory and Atmosphere Reconstruction," *48th AIAA Aerospace Sciences Meeting*, January 2010, AIAA Paper 2010-1210.

[16]Molavi, H., Hakkaki-Fard, A., Pourshaban, I., Mahbubi Fard, M., and Rahmani, R. K., "Estimation of Temperature-Dependent Thermophysical Properties of Noncharring Ablator," *Journal of Thermophysics and Heat Transfer*, Vol. 23, No. 1, 2009. pp. 50-58.

[17]Beck, J.V., "Transient Determination of Thermal Properties," Nuclear Engineering and Design, Vol. 3, No. 3, 1966, pp. 373–381.

[18]Sawaf, B., Özisik, M.N., and Jarny, Y., "An Inverse Analysis to Estimate Linearly Temperature Dependent Thermal Conductivity Components and Heat Capacity of an Orthotropic Medium," *International Journal of Heat and Mass Transfer*, Vol. 38, No. 16, 1995, pp. 3005–3010.

[19]Huang, C.H., and Yan, J.Y., "An Inverse Problem in Simultaneously Measuring Temperature-Dependent Thermal Conductivity and Heat Capacity," *International Journal of Heat and Mass Transfer*, Vol. 38, No. 18, 1995, pp. 3433–3441.

[20]Dantas, L.B., and Orlande, H.R.B., "A Function Estimation Approach for Determining Temperature-Dependent Thermophysical Properties," *Inverse Problems in Engineering*, Vol. 3, No. 4, 1996, pp. 261–279.

[21]Dowding, K.J., Beck, J.V., and Blackwell, B.F., "Estimating Temperature-Dependent Thermal Properties," *Journal of Thermophysics and Heat Transfer*, Vol. 13, No. 3, 1999, pp. 328–336.

[22]Garcia, S., "Experimental Design Optimization and Thermophysical Parameter Estimation of Composite Materials Using Genetic Algorithms," Ph.D. Dissertation, Dept. of Mechanical Engineering, Virginia Polytechnic Inst. and State Univ., Blacksburg, VA, USA, 1999.

[23]Oliveira, A.P.D., and Orlande, H.R.B., "Estimation of the Heat Flux at the Surface of Ablating Materials by Using Temperature and Surface Position Measurements", *Inverse Problems in Science and Engineering*, Vol. 12, No. 5, 2004, pp. 563 577.

[24]Kanevce, L. P., and Kanevce, G. H., "Comparison of two kinds of experiments for estimation of thermal properties of ablative composite", *3rd int. Conference on Inverse Problems in Engineering*, 1999.

[25]Silva, D. V. F. M., and Orlande, H. R. B., "Estimation of Thermal Properties of Ablating Materials" *Inverse Problems in Science and Engineering III*, 2002, pp. 49-58

[26]Özisik, M. N., and Orlande, H. R. B., *Inverse Heat Transfer: Fundamentals and Applications, Taylor and Francis, New York, 2000.*

[27]Beck, J. V., and Arnold, K. J., *Parameter Estimation in Engineering and Science, Wiley, New York, 1977*.